Femtosecond laser micromachining of Integrated Circuits (ICs) for semiconductor defect analysis

M. Halbwax[*], T. Sarnet[*], J. Hermann, Ph. Delaporte[*], M. Sentis[*]
L. Fares[**], G. Haller[**]

[*]Laboratoire LP3 CNRS UMR 6182 Luminy Marseille, France
[**]STMicroelectronics, Rousset, France

ABSTRACT

Integrated Circuits have been cross-sectioned with a femtosecond laser for defect analysis purpose. This study shows the influence of the irradiation conditions (pressure, polarization, optics, energy density, scanning parameters...) on the quality of the laser microcutting.

Keywords: laser microcutting, engraving, femtosecond laser, defect analysis.

1 INTRODUCTION

The detection and analysis of defects in Integrated Circuits (ICs) are major challenges faced by the semiconductor industry as outlined by the roadmap in the latest International Technology Roadmap for Semiconductors (ITRS 2005) [1].

Advanced tools used today for defect cross sectioning include dual beams (focused ion beam and scanning electron microscope FIB/SEM) with resolution down to the sub-Angstrom level.

However ion milling an IC with a FIB is time consuming because of the need to open first wide cavities in front of the cross-sections that need to be analyzed. Therefore the use of a femtosecond laser as a tool for direct material removal is discussed in this paper. Experiments were performed on IC structures to reveal the different layers of fabrication: depending on the laser energy density a selective or total ablation of the materials can occur, without delamination of the layers. Different laser irradiation conditions like pressure (air, vacuum…), polarization, beam shaping, scanning parameters and energy density have been used to produce different types of cavities. The femtosecond laser engraving of silicon-based structures could be useful for cross-sectioning of devices but also for other applications like direct-write lithography, photomask repair, maskless implantation or reverse engineering/restructuring.

2 EXPERIMENTAL SET-UP

The samples were p-type Si(001) cleaved wafers and ICs fabricated at STMicroelectronics Rousset, France.

The engraving of the samples was carried out in a vacuum chamber with a pressure of $5x10^{-5}$ to $1x10^{-5}$ mbar. This low pressure considerably reduces the redeposition of unwanted debris from the laser ablation process [2].

The optical set-up that was used to deliver the laser beam to the sample surface is presented in Figure 1 [3]. The micromachining experiments was performed using a Ti:sapphire laser (Hurricane model, Spectra-Physics) at 800 nm, 500 µJ energy, 1 kHz repetition rate and a laser pulse duration of 100 fs. To get a more uniform laser energy distribution, only the center part of the gaussian laser beam was selected using a square mask (D) of 2 x 2 mm^2.

A computer-controlled XY-stage (for the sample) and Z stage (for the objective lens) has allowed precise positioning of the spot on the surface sample. The laser energy that was delivered to sample surface could be attenuated by using a combination of analyzer (A) and polarizer (P) and completed by a set of neutral density filters (NDF). A PC controlled the analyzer rotation, as well as the opening and closing of shutter (S) placed in front of the polarizer, and the XYZ stages. The engraving results are *in situ* monitored by a CCD camera.

Different spot sizes were obtained by projecting the mask image onto the sample surface with a planoconvex lens (f' 50 mm). By moving the lens along the z axis, different spot sizes and shapes were obtained.

We also used a microscope long working distance objective (Carl Zeiss, Epiplan, 50x/0.50) to focus the gaussian laser beam: in that case the spot on the sample surface was circular with a diameter ~3 µm.

50 x 250 $µm^2$ surfaces have been irradiated by scanning a simple straight line at a velocity of 150 µm/s, with a 1 µm shift between the scans to treat the whole surface. For each microcavity, this process was repeated 10 times (10 runs). The completion time was therefore 30 minutes for each microcavity.

The experiments were carried out at different fluences ranging from 200 to 6500 mJ/cm^2.

The engraving and topography were characterized using Scanning Electron Microscopy (SEM) and Optical Microscopy (OM) in dark field mode. The heat affected zone and eventual damage were observed on cross sections by Transmission Electron Microscopy (TEM CM 200 Philips, 200 kV). The cross sections were prepared by Focused Ion Beam milling (FIB FEI Strata DB-STEM 237).

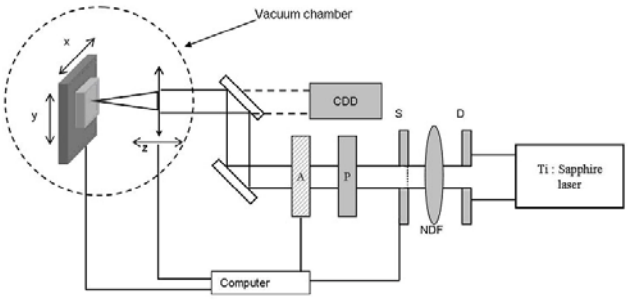

Figure 1: diagram of the femtosecond laser experimental set-up

3 RESULTS AND DISCUSSION

In order to optimize the translation of the beam with respect to its linear polarization, we have made long trenches (6 mm) on Si(001) according to 2 different axes: the laser spot displacement was perpendicular (along y axis) and parallel (along x axis) to the axis of polarization. The sample surface was positioned to the f'50 mm lens focal plane. The Figure 2 shows the engraving results of cleaved samples. The best results have been obtained with a beam translation perpendicular to the polarization: in that case the trench is clean and symmetrical (Figure 2a). Using a spot translation parallel to the polarization did not give nice laser cuts (Figure 2b): the trench was not symmetrical, with a typical comma shape. In that case the absorption of the laser beam is not optimal: these results are consistent with previous studies [4]. For this study, the structures were realized with a spot displacement perpendicular to the polarization.

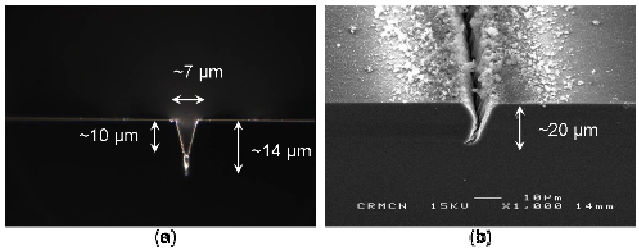

Figure 2: (a) Optical microscope view (Dark Field) of a trench with beam translation perpendicular to the polarization and (b) SEM view of a trench with beam translation parallel to the polarization

We realized several microcavities with different spot sizes and fluences ranging from 150 to 2000 mJ/cm^2. We observed that the angle between the sample surface and the microcavities walls increased when decreasing the spot size. For example, we obtained a 70° angle when the sample was positioned to the mask image plane, with a 35 µm spot, and a maximum of 75° when the sample surface was located in the lens focal plane, with a 15 µm spot. We observed that the fluence has not significant effect on the angle variation.

In order to get a more abrupt wall, we used the microscope objective (x50) as a focusing optics which allowed a 3 µm spot size. In that case we obtained microcavities walls with a 90° angle.

The results of this study have shown that, for Si(001) , engraving at low fluence (< 250 mJ/cm^2) is preferred to minimize the particle redeposition coming from the laser engraving process. However using such a low fluence is not suitable for the total engraving of an IC. Indeed, the micro-chips contain dielectrics like nitrides and refractory metals like tungsten which are not engraved at these low fluences [5-6]. For some dielectrics, a fluence of several J/cm^2 was necessary for a total engraving of the structures [7]. However, in some cases engraving an IC at low fluence (250 mJ/cm^2) could be interesting: a selective engraving of materials occurs that reveals structures like vias. This selective engraving process is interesting for reverse engineering/restructuring applications.

In order to engrave the totality of the various materials composing the circuit multi-layers, we had to choose a rather strong fluence: 6.5 J/cm^2.

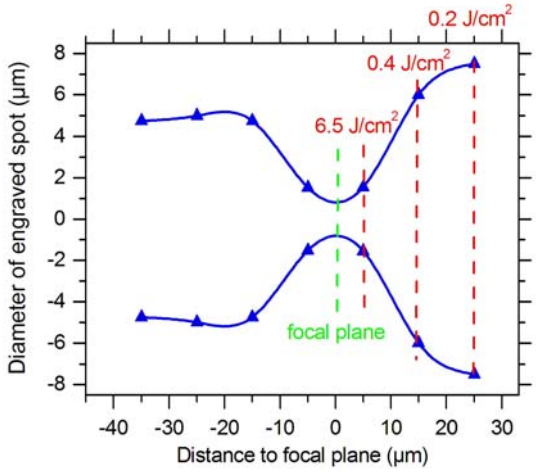

Figure 3: diameter of the engraved spot as a function of the distance to the focal plane. Incident energy ~ 500 nJ

The Figure 3 shows the diameter of the engraved spot as a function of the distance (z_f) to the focal plane (along z axis) with an incident energy of about 500 nJ. The observed divergence of the beam after the focal plane is due to the low depth of field (DOF) of the microscope objective. This implies a rapid variation of the fluence as a function of z_f. If

z_f is equal to 5 µm we obtain a fluence of 6.5 J/cm^2, this fluence decreases down to 0.4 J/cm^2 for z_f = 15 µm.

For the microcavity engraving, we have placed the sample surface at z_f = 5 µm to get a fluence of 6.5 J/cm^2 on the top surface. In order to avoid the high redeposition problem, we developed an engraving process in three steps. The first run is effectively used for engraving (~ 15 µm depth), but implies a large amount of redeposition (Figure 4a). For the following runs, the engraving rate is lower because of the laser beam divergence. Indeed, after 15 µm of engraving, the fluence decreases down to 300 mJ/cm^2. This decrease in energy density has two major benefits: firstly, the additional runs produce very little redeposition and secondly, each following run eliminates some redeposited particles from the previous run, as shown in Figure 4b and 4c. After engraving 20 µm (Figure 4c), the process is almost completed, the fluence becomes too small to engrave anymore. In a third step, a series of final runs is performed to clean the surface by removing the redeposited particles (Figure 4d).

The low DOF of the optics implies a strong laser beam divergence after the focal plane: this allows a self-regulation of the fluence.

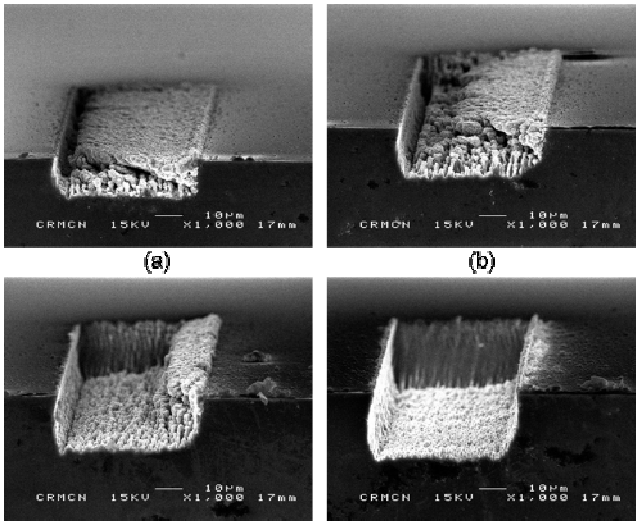

Figure 4: SEM images of engraved silicon microcavities after (a) one run, (b) two runs, (c) six runs and (d) ten runs. Surface fluence = 6.5 J/cm^2

After validating the process, we have engraved real ICs from ST Microelectronics. These chips are composed of many overlapping layers of various materials (metals, dielectrics…, 5-7 µm total thickness) on a silicon substrate. Figure 5 shows the engraving results on a chip. We observed microcavities with abrupt walls and only a small amount of redeposition at the bottom and outside the cavities. The roughness observed at the bottom of the microcrocavity is due to the formation of erected structures [8]: this roughness can be rather high (10 µm spikes) but it is limited to the bottom of the cavity and is not critical for the FIB milling.

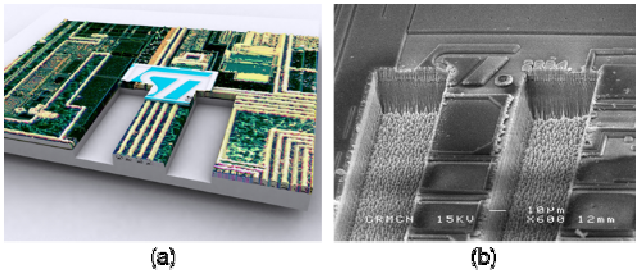

Figure 5: (a) 3D Computer Generated Image of the engraving and (b) SEM image of engraved microcavities in STMicroelectronics IC

TEM cross-sections of engraved microcavities walls in Si(001) substrate have revealed two distinct zones of defects (F=250 mJ/cm^2). The first region consists in an amorphized silicon layer with a thickness ranging from 20 nm (Figure 6) to 100 nm. Below this amorphous layer, the silicon crystal seems to be damaged on a 200 nm thickness. Additional cross-sections need to be analyzed by TEM for samples engraved at higher fluences (F>250 mJ/cm^2), however we presume that the damaged region is still quite small (sub-micron scale).

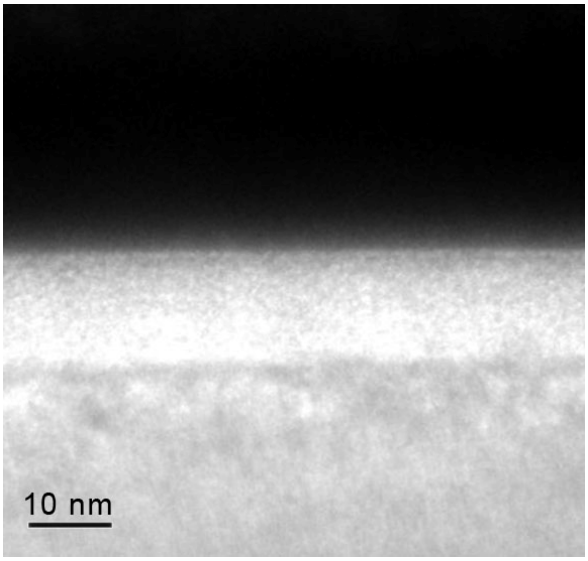

Figure 6: Cross-sectional TEM image of a microcavity wall surface: top layer shows the 20 nm amorphized silicon.

These results are very interesting to prepare cross-sectional thin foil for TEM observation. Figure 7 schematizes the steps of a milling process that include the femtosecond laser engraving. This laser engraving allows the opening of the wide cavities and the thinning of the center wall down to a micrometer scale: the FIB milling is therefore limited to the finishing steps. Since the

micrometric wall is reduced down to a 150 nm thickness by FIB milling, the laser damaged zone is suppressed by the FIB. One advantage of the laser process is that the engraving speed is much faster than FIB milling.

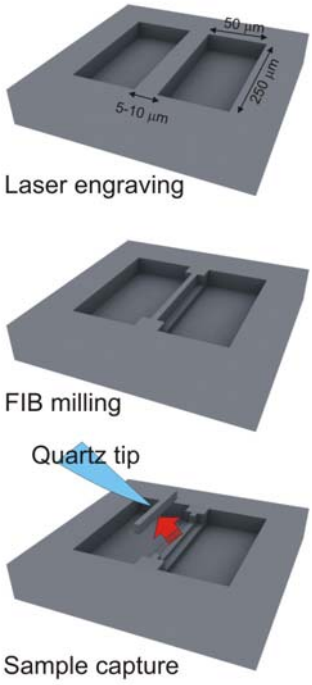

Figure 7: Steps of thin foil realization for TEM observation

4 CONCLUSIONS

We have used a femtosecond laser as a tool for direct material removal for semiconductor defect analysis.

After investigating the influence of the different laser-matter interaction parameters (pressure, polarization, beam shaping, scanning parameters, energy density...) on the quality of the engraving, we have developed a self-regulation engraving process, in which the ablation automatically stops when the cavity is finished and cleaned. This process allows the rapid engraving of cavities with abrupt walls, submicrometric damaged zone and without redeposition in the treated area.

This localized engraving is very interesting for FIB milling because it drastically reduces the milling process time. But other applications are also possible like the engraving of microstructures without lithography steps (direct-write lithography), photomask repair or maskless implantation. However, the laser engraving of monocrystalline silicon implies a modification of the surface morphology with an increase in roughness that depends on the laser irradiation conditions. This roughness is not acceptable for some applications like MEMS. Therefore an additional process has to be done to smooth the surface, like excimer laser planarization [9] or chemical etching [10]. Additional experiments are also being carried out at LP3 to include the femtosecond laser engraving in the technological steps for microstructure realization like microbridges [11-12].

ACKNOWLEDGMENTS

This work has been mainly supported by STMicroelectronics ROUSSET, but also by the City of Marseilles, PACA and CG 13 in the framework of PIALA (Plate-forme Interdisciplinaire Ablation Laser et Application). The authors thank S. Nistche, D. Chaudanson and L. Beauvisage for their help concerning the SEM and TEM observations.

REFERENCES

[1] Technology Roadmap for Semiconductors (ITRS), Process Integration, Devices & Structures Topic, www.itrs.net, 2001

[2] J. Hermann, M. Benfarah, S. Bruneau, E Axente, G. Coustillier, T. Itina, J. –F Guillemoles and P. Alloncle, J. Phys. D: Appl. Phys. 39, 453, 2006

[3] S. Noël, J. Hermann and T. Itina, "Investigation of nanoparticle generation during femtosecond laser ablation of metals", Appl. Surf. Sci, In Press, Accepted Manuscript.

[4] T. H. R. Crawford, A. Borowiec and H. K. Haugen, Appl. Phys. A. 80, 1717, 2004

[5] P. Rudolph and W. Kautek, Thin Solid Films 453/454, 537, 2004

[6] L. Urech, T. Lippert, A. Wokaun, S. Martin, H. Mädebach and J. Krüger, Appl. Surf. Sci. 252, 4754, 2006

[7] A-.C Tien, S. Backus, H. Kapteyn, M. Murnane and G. Mourou, Phys. Rev. Lett. 82, 3883, 1999

[8] M. Halbwax, T. Sarnet, Ph. Delaporte, M. Sentis, H. Etienne, F. Torregrosa, V. Vervisch, I. Perichaud and S. Martinuzzi, "Ultra-short pulsed laser for nano-texturization associated to plasma immersion implantation for 3D shallow doping: Application to silicon photovoltaic structures" submitted to Journal of Experimental Nanoscience 2007

[9] A. Bosseboeuf, J. Boulmer and D. Debarre, Appl. Surf. Sci. 110, 473, 1997

[10] J. M. Lysko, Mater. Sci. Semicond. Process. 6, 235, 2003

[11] T. Sarnet, G. Kerrien, N. Yaakoubi, A. Bosseboeuf, E. Dufour-Gergam, D. Débarre, J. Boulmer, K. Kakushima, C. Laviron, M. Hernandez, J. Venturini and T. Bourouina. Appl. Surf. Sci. 247, 537, 2005

[12] P. Goudeau, N. Tamura, B. Lavelle, S. Rigo, T. Masri, A. Bosseboeuf, T. Sarnet, J. A. Petit, J. M. Desmarres. Mater. Res. Soc. Symp. Proc. 875, 121, 2005